JOURNAL OF MATERIALS SCIENCE 22 (1987) 4281–4291

An experimental study of synthetic fibre reinforced cementitious composites

YOUJIANG WANG*, STANLEY BACKER*, VICTOR C. LI‡
*Department of Mechanical Engineering and ‡Department of Civil Engineering, Massachusetts Institute of Technology, Cambridge, Massachusetts 02139, USA

Fibre reinforcement is one of the effective ways of improving the properties of concrete. However, current studies on fibre-reinforced concrete (FRC) have focused mainly on reinforcements with steel and glass fibres. This paper reports on an experimental programme on the properties of various synthetic fibre reinforced cementitious composites and the properties of the reinforcing fibres. Acrylic, polyester, and aramid fibres were tested in uniaxial tension, both in their original state as well as after ageing in cement. Samples of these fibres were found to lose varying amounts of strength with time, depending on the ageing temperature. Two different test methods were used to measure the fibre–cement interfacial bond strength. The tensile properties of concrete reinforced with acrylic, nylon, and aramid fibres, in the form of random distribution or uniaxial alignment, were studied by means of three different tests: compact tension, flexural, and splitting tensile tests. The properties of concrete, particularly that of apparent ductility, were found to be greatly improved by the inclusion of such fibre reinforcement.

1. Introduction

In recent years, the decay in infrastructures has come to be seen as a national crisis [1]. Estimates have put the cost of repair and rehabilitation at 1 to 3 $\times$ 10^{12} US dollars over the next twenty years [2]. Many of the decay problems require a good dosage of proper management and maintenance. However, the intrinsic cause of the crisis is the deterioration of the material used in the original construction, and in subsequent repairs, in response to mechanical and environmental loads. Severity of loading is not expected to decrease. In fact, for highway systems, current policies in the USA encourage a continued increase in truck tyre pressures (moving up from 90 p.s.i. (620 kPa) to 120 to 150 p.s.i. (827 to 1034 kPa)) which will clearly increase the traffic loads. And this at a time when our highway systems are beginning to manifest clear signs of ageing and deterioration.

The deterioration of infrastructures may manifest itself as cracking, spalling and scaling, which suggests a lack of resistance to tensile loads in concrete, even when reinforced by re-bars. Fibre reinforcement has been proven to be an effective and economical way to improve the properties of concrete. Asbestos cement has been successfully employed in factory-prefabricated elements for nearly a century [3], and is in extensive use all over the world. Recently its use has been curtailed for health reasons. Research on FRC using other fibres has been carried out in the past two decades and great progress has been achieved. Fibres such as steel, glass, nylon, polypropylene, polyethylene, aramid, carbon, polyester, acrylic, and various natural fibres, have been used in FRC and some of these materials are in commercial production [4–9]. Recently, ASTM has approved a standard for steel fibres for FRC [10] and a standard for FRC flexural toughness measurement [11]. American Concrete Institute (ACI) has also approved a guide for fabricating steel FRC [12].

FRC is used for many applications, for instance in the construction industry, as highway and airport runway overlays, nuclear reactor shieldings, pile caps, tunnel wall linings and refractory materials, and in the building industry as pipes, flat and corrugated sheets, roof, floor and decorative panels [4, 13–15]. Some very recent applications include the guideway for a new transit system on Kobe Port Island in Japan, and in the rehabilitation of damaged waterways. Apart from crack resistance improvements, some of the advantages of FRC over conventional concrete include lightweightness, such as in glass FRC for building panels which result in reducing the cost and size of the supporting structural members, improved load-carrying capacity, greater allowable distance between shrinkage joints for industrial flooring, and improved impact energy absorption and wear durability for airport taxiways.

This paper describes an initial experimental programme to study the feasibility of using synthetic polymeric fibres as the reinforcement in the composite. The choice of polymeric fibres is encouraged by the technological sophistication of the synthetic fibre industry, which has made available a wide range of fibres of very low to extremely high tensile moduli. Such fibres can be made in a variety of cross-sections and with specially designed surface finishes. Our preliminary work based on selected currently available polymetric fibres has shown that this fibre

0022–2461/87 $03.00 + .12

reinforcement holds great promise in improving the ductility of plain concrete and cement. Synthetic fibre reinforced concrete may become a very attractive construction material in the future.

In this paper, we shall first describe the various fibres we have used in this experimental programme, as well as their physical and mechanical properties. The experimental set-up and test results for fibre–cement interfacial bond strength and for fibre stability will be described. This is followed by a presentation of composite tensile behaviour based on tests in compact tension, flexural, and splitting tensile specimens. Our intention is to use these test results as a fundamental database from which we do further experimental and theoretical analysis of the properties of synthetic fibre reinforced cementitious composites.

2. Materials

Portland cement Type III, a high-early-strength cement, and silica sand No. 45 were used throughout the programme to form the matrix of FRC. The weight ratio of cement : sand : water was kept at 1 : 1 : 0.5 unless otherwise specified. Acrylic, nylon, and aramid fibres were used as reinforcing fibres. The acrylic, polyester, and nylon fibres were furnished through courtesy of E.I. du Pont de Nemours & Co. The aramid fibre was obtained by cutting a continuous filament yarn employed in another experimental programme, and does not represent the current commercial aramid products of the DuPont company.

3. Fibre properties

Staple acrylic, polyester, nylon and aramid fibres, and continuous acrylic filaments, and their interactions with cement matrix were studied.

3.1. Tensile properties

Fibre tensile properties were measured by a single-fibre tension test, performed on an Instron machine using a special fibre fixture. A fibre gauge length of 35 mm and a crosshead speed of 12.7 mm min^{-1} (0.5 in min^{-1}) were used for acrylic and polyester fibre tension tests. The aramid fibres were tested with a gauge length of 127 mm (5 in) and a crosshead speed of 12.7 mm min^{-1} (0.5 in min^{-1}). For tests of nylon fibres, a gauge length of 254 mm (10 in) and a crosshead speed of 127 mm min^{-1} (5 in min^{-1}) were used. For each fibre, a tension–elongation curve was recorded. Fibre ultimate strength, elongation to rupture and initial modulus were calculated and are reported in Table I. The fibre cross-sectional dimension, strength and initial modulus are given in SI units as well as in denier or grams per denier (g.p.d.)*, as the latter unit system is commonly used in the synthetic fibre industry. From the viewpoint of dimensions, the stress unit g.p.d. is expressed in length (m), which, for breaking stress, corresponds to the fibre breaking length. Fig. 1 shows some typical fibre tensile test curves (for end-point for aramid fibre, see Table I). These synthetic fibres, with the exception of the aramid, show great non-linearity in stress–strain behaviour. The aramid fibre tested exhibited a lower elastic modulus and higher elongation to break, compared with the aramid fibre Kevlar 49 [6].

3.2. Fibre chemical stability

The durability of FRC is very important because concrete constructions are generally designed to last several decades. This requires the constituents of FRC to remain chemically stable over a long period under service conditions. The major components of Portland cement are calcium silicates and aluminates. In the presence of water, hydration and hydrolysis reactions take place, resulting in a strongly alkaline solution (pH 10 to 12) of calcium hydroxide [$Ca(OH)_2$]. Some fibres (e.g. glass) lose their strength gradually when mixed with cement.

Nylon, polypropylene, and polyethylene fibres are very resistant to alkalis [16] and no degradation of these fibres in cement has been found [17, 4]. Acrylic, polyester, and aramid fibres are not resistant to some strong alkalis [16]. Unfortunately, information available in the literature concerning their stability in FRC is insufficient or inconsistent. For example, Jakel [8] claimed success in using polyester fibres to improve Portland cement products, but ACI Committee 544 [4] concluded that polyester and acrylic fibres are ineffective as reinforcement in Portland cement products, due to their chemical degradation in cement. Walton and Majumdar [6] evaluated the durability of

TABLE I Fibre tensile properties

Fibre	Denier	d_f (μm)	Strength			Elongation (%)	Initial modulus		Fibres tested
			g.p.d.	GPa	CV (%)*		g.p.d.	GPa	
Acrylic†	3.0	19.2	2.9	0.3	10.7	12.6	54.6	5.5	39
Acrylic‡	3.0	19.2	6.0	0.6	13.1	13.3	100.6	10.2	43
Polyester§	5.2	23.1	9.4	1.1	4.4	24.4	83.3	10.0	12
Aramid§	1.5	11.9	24.5	3.2	12.6	4.1	552.5	73.1	20
Nylon§	6.0	27.2	9.5	1.0	10.3	15.8	57.8	5.8	11
Cement¶				0.01		0.04		20	

*CV = coefficient of variation (standard deviation/average).
†Staple fibres.
‡Continuous filaments from tow.
§Cut from continuous filament yarn.
¶Included for comparison.

*Conversions: 1 denier = 9000 × (linear density, g m^{-1}); fibre diameter (d_f) = [4 × denier / (9000$\pi\gamma$)]$^{1/2}$ mm and 1 g.p.d. = 0.08826γ GPa, where γ is the fibre density (g cm^{-3}).

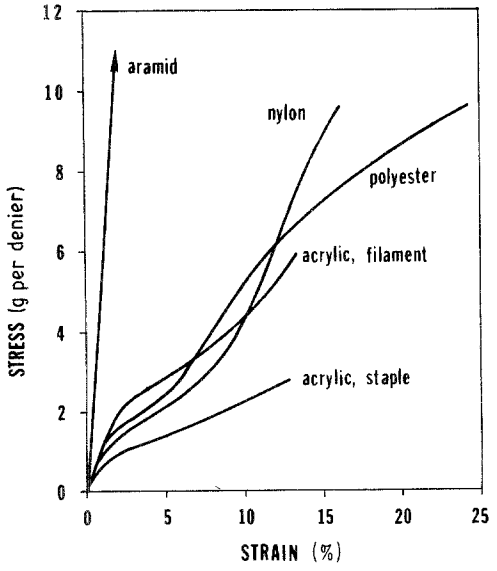

Figure 1 Tension test curves for fibres.

aramid (Kevlar 49) FRC based on strength tests of composite specimens aged for up to two years at ambient temperatures. Their test results indicated good durability of such composites.

In the light of these uncertainties, we have undertaken ageing-in-cement stability tests for selected specimens of polyester, acrylic, and aramid fibres. The matrix for this testing was made of two parts of cement and one part of water (weight fractions), hand-mixed into a homogeneous cement paste. The specimen was prepared by putting a fibre bundle surrounded by the cement paste into a Plexiglas box. Specimens were stored in a 100% relative humidity (RH) environment at a temperature of 22 or 50° C for a specified period. The fibre bundles were extracted by splitting the matrix. Only the fibres in the centres of the bundles were kept for testing, in that they were exposed to alkaline conditions of ageing in cement, but were not individually embedded so as to be damaged during extraction. Tests on the aged fibre specimens were performed as for fibres in the original, as-received state. The breaking strength of fibres so exposed relative to that of new fibres, the strength ratio, is plotted as a function of time in Fig. 2. From these results it can be seen that polyester fibres lose strength rapidly in the cement matrix. The strength of the aramid fibres also drops in cement, especially at a higher temperature (50° C). The data for the stability of acrylic fibres at room temperature (22° C) indicate a slight decrease in average strength with age in cement, but the strength loss of acrylic fibres aged in cement at 50° C is significant. These results are consistent with reports that polyester, acrylic, and aramid fibres are not resistant to strong alkalis [16].

It should be pointed out that since the aged fibres tested were not in direct contact with the cement matrix, the degradation of other fibres in direct contact with the cement matrix might have been more severe than that indicated by Fig. 2.

Based on the data showing the strength degradation of cement-embedded polyester, aramid, and acrylic fibres, the question must be raised as to the suitability of these fibres for reinforcing Portland cement based composites. It should be emphasized that only one particular sample of these generic fibre types was evaluated and the test results cannot be quantitatively applied to the numerous fibre modifications commercially available in each generic group. None the less, the findings emphasize the importance of determining the "in-matrix" strength stability in selecting fibres for cement reinforcement, unless such fibres are to be used in non-alkaline cement materials.

3.3. Bond strength

Bond strength and shear stress transfer mechanisms are very important factors affecting the properties of FRC. This is obvious because any contribution from the discrete fibres to the composites has to be transferred via the fibre–matrix bond. Bartos [18] reviewed the characteristics, test methods and test results for fibre–matrix bonding in FRC. Most tests reported in the past have been conducted on steel and glass fibres, with very few on other fibres. In this study, the average shear bond strength with cement for acrylic, aramid, polyester and nylon fibres were measured.

The conventional established methods for determining the bond strength for thick and stiff fibres [18, 19] are not considered to be suitable for thin flexible synthetic fibres because of the difficulties in putting fibres in the matrix in a prescribed manner.

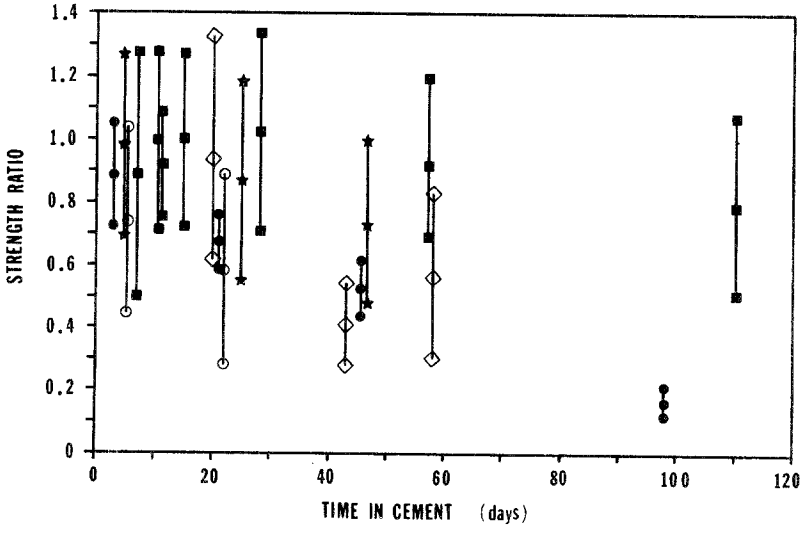

Figure 2 Fibre strength variation with age in cement (bars represent average ±2 standard deviations). (■) Acrylic, 22° C; (◇) acrylic, 50° C; (★) aramid, 22° C; (●) aramid, 50° C; (○) polyester, 22° C.

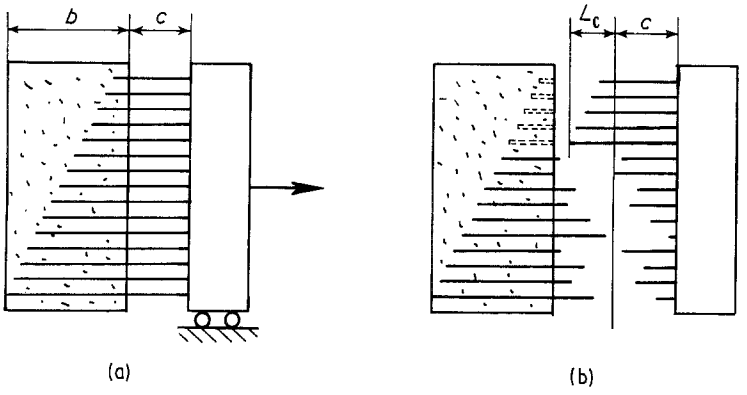

Figure 3 Bond strength determination by the critical length (L_c) method: (a) before pull-out, (b) after pull-out. b = 19.5 mm, c = 10 mm.

In this study two methods were used to measure the fibre–matrix bond strength for synthetic fibres.

1. Critical Length (L_c) method. This method is based on the critical length of fibre pull-out, which is particularly suitable for very thin, high bond strength fibres, for which bond strength is very difficult to measure otherwise. However, only the peak value of the average bond strength over a certain fibre length can be determined by this method, which depends on the uniformity of the fibre breaking strength. The schematic diagram for the test set-up is shown in Fig. 3. An array of fibres with successive lengths was planted in a cement matrix. After a given curing time, the fibre array was pulled out at a speed of 12.7 mm min^{-1} (0.5 in min^{-1}), and the critical length L_c was obtained directly by measuring the maximum length of fibres pulled out without rupture. The average bond strength can then be calculated from

$$\tau = d_f \sigma_f / 4L_c$$

where d_f is the fibre diameter and σ_f is the fibre ultimate strength (in units of stress). For fibres showing deterioration in the cement matrix, breaking stress values were based on the data presented in Fig. 2.

2. Direct method. In this method fibres were put in the cement matrix as shown in Fig. 4. After a given curing period, the fibres were pulled out by an Instron machine at 12.7 mm min^{-1} (0.5 in min^{-1}) one by one. Results can only be obtained when the fibre critical length L_c exceeds the thickness of the cement specimen (b in Fig. 4). The average bond strength τ was then determined from the load P and the geometric dimensions:

$$\tau = P/\pi d_f b$$

For both methods the cement matrix was made from a hand-mixed cement paste containing two parts of cement and one part of water (weight fractions). The moulds for the specimens were 15 mm × 19.5 mm × 43 mm) Plexiglas boxes, whose sides were removed by cutting one day after casting. All the specimens were cured in a 100% RH environment at room temperature (22° C) for a prescribed period.

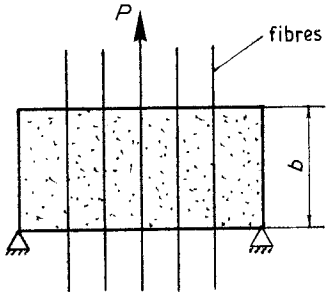

Figure 4 Specimen for the direct method for bond strength determination. b = 19.5 mm.

Test results of the average shear strength of the fibre–cement interfacial bond are given in Table II. The actual bond strengths (maximum shear stress) are, however, expected to be higher than the indicated average values. Because the same moulds were used for both methods in this study, the specimen lengths b in Figs 3a and 4 are identical. Hence the L_c method (Fig. 3) was usable only for fibres whose critical length L_c was less than the length b, and the direct method (Fig. 4) for fibres with $L_c > b$. As a result, a comparison of average bond strengths based on the two methods cannot be made at this time.

A very low bond strength between nylon fibres and the cement matrix was observed, which was consistent with the results reported in the literature [20]. Acrylic fibres formed a very strong bond with the cement matrix. Because the critical length of pull-out (L_c) for acrylic fibres was so short (about or less than 1 mm), an accurate measurement was not obtained. A high bond strength with the cement matrix was also found for aramid fibres and a low bond strength for polyester fibres. The bond strengths varied with age in cement, probably because the fibre surfaces were attacked by the cement alkalis and were roughened as a result. This finding is in agreement with the results of those fibre stability tests which indicate strength loss in fibres embedded in cement.

4. FRC tests

The properties of FRC reinforced with synthetic fibres were studied by flexural, splitting tensile and compact tension specimen (CTS) tests.

4.1. Specimen preparation

Random fibre reinforced concrete beams were formed by first mixing cement, sand and water in a concrete mixer for a few minutes, then adding fibres and continuing mixing for another few minutes. The mixture usually did not have "pouring fluidity" and had to be formed into moulds by hand. For some specimens fibres were straightened and laid in the longitudinal direction of the moulds, layer by layer. The reusable beam moulds were made of Plexiglas plates, sealed

TABLE II Fibre–cement bond strength

Fibre	Denier	d_f (μm)	σ_f (GPa)	Method	Age (days)	P (N)	L_c (mm)	τ (MPa)
Nylon	6.0	27.2	0.96	Direct	12	0.273		0.16
Acrylic*	3.0	19.2	0.61	L_c	3		~1.0	2.93
Aramid	1.5	11.9	3.18	L_c	3		4.9	1.93
			2.96	L_c	17		3.2	2.75
Polyester	5.2	23.1	1.08	Direct	1	0.175		0.11
			0.84	Direct	5	0.269		0.14
			0.78	L_c	12		15.5	0.29

*Continuous filaments from tow.

with caulking compound. The size of the beams was 102 mm × 102 mm × 356 mm (4 in × 4 in × 14 in), which was suggested by ACI Committee 544 for FRC flexural strength and toughness tests [21]. In each test set, eight beams were cast, including two or three controls containing no fibres.

The specimens in the moulds were put into plastic bags for setting, then were removed from the moulds one day later, and put back into plastic bags for curing. The environment in the bags was about 100% RH and about 22° C (room temperature).

Compact tension specimens were made by slicing the beams and then drilling the loading holes and cutting the slits. The configuration and dimensions of the CTS used in this study are shown in Fig. 5. The root of the crack was cut with a diamond saw of 0.8 mm thickness. The crack length a was about 38 mm (1.5 in).

Four-point bending tests were performed directly on the beams, and the undamaged portions of the beams tested in flexure were subsequently used in the splitting tensile tests.

The sizes of the beams and the CTS specimens may vary by a small amount (< 2%) from the nominal values due to errors in specimen preparation. The calculations used the actually measured dimensions of each specimen.

Twelve batches of FRC specimens with different fibre types, geometries or volume fractions and ten batches of associated control specimens have been prepared and tested, including 97 compact tension specimens and 46 beams. The mix details are given in Table III.

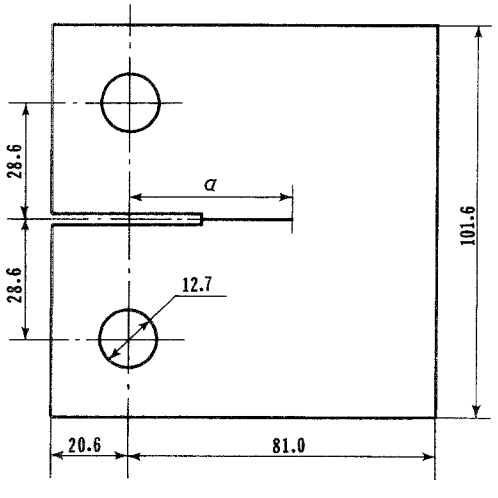

Figure 5 Dimensions (mm) of the compact tension specimens. Thickness B = 50.8 mm.

4.2. Compact tension test

Compact tension specimens were tested on an Instron machine at a crosshead speed of 0.5 mm min^{-1} (0.02 in min^{-1}). A clip gauge was attached to the specimen crack mouth to measure the load-line displacement directly. The load against load-line displacement curves were recorded with an X–Y plotter. Load against crosshead displacement curves were also recorded, by means of the autographical device of the testing machine.

From the load against load-line displacement curves, the toughness of FRC was measured in terms of a pair of quantities: the limit of proportionality (LOP) toughness, T_0, and the dimensionless toughness index, DTI_{20}, as defined below with reference to Fig. 6:

$$T_0 = S_0/A \ (\mathrm{J\,m^{-2}})$$

$$DTI_{20} = (S_0 + S_1)/S_0$$

where S_0 and S_1 are portions of the area under the load–displacement curve as indicated in Fig. 6, and A is the projected area of specimen fracture surface.

This method of measuring the toughness of FRC has been found to be more reasonable than the conventionally used toughness quantities [22, 23]. While this measure of toughness may be size- and geometry-dependent, it should nevertheless provide a simple, inexpensive quantitative measure for ranking the toughness of materials when tested with the same specimen geometry, size and loading conditions. The LOP toughness, T_0, is an indication of the matrix toughness, while DTI_{20} represents the improvements in energy-absorbing ability of FRC due to fibre inclusion.

Results of the compact tension test are summarized in Table IV. Fig. 7 shows two test curves recorded simultaneously by different methods for the same FRC specimen. One of the curves is plotted as the load against crosshead movement, and the other is load against load-line displacement measured at the crack mouth by a clip gauge. The significant difference between these curves indicates that the deformation of the test equipment (test fixture and the testing machine) cannot be neglected in CTS tests, and that a direct measurement of the load-line displacement is necessary.

The results in Table IV were obtained from the load against load-line displacement curves. The LOP point (point at the limit of proportionality), which was used to calculate the toughness quantities, was determined

TABLE III Mix details for test specimens

Mix No.	Fibre	V_f (%)	L_f (mm)	Denier	d_f (μm)	Crimp	Test age (days)	
							CTS	Bending
C1	None	0.0	–	–	–	–		92
A1	Acrylic	2.4	25.4	1.5	13.6	None		92
C2	None	0.0	–	–	–	–		120
A2	Acrylic	2.4	38.1	1.5	13.6	None		120
C3	None	0.0	–	–	–	–	33	
K1	Aramid	1.9	25.4	1.5	11.9	None	33	
A3*	Acrylic	6.5	6.4	3	19.2	None	33	
C4	None	0.0	–	–	–	–	47	
A4	Acrylic	2.0	6.4	3	19.2	None	47	
A5	Acrylic	4.0	6.4	3	19.2	None	47	
C5	None	0.0	–	–	–	–	38	131
A6	Acrylic	2.0	12.7	1.5	13.6	None	38	131
C6	None	0.0	–	–	–	–	51	111
A7	Acrylic	2.0	19.1	3	19.2	Yes	51	111
C7	None	0.0	–	–	–	–	43	146
A8†	Acrylic	4.5	Tow	3	19.2	None	43	146
C8	None	0.0		–	–	–	59	
N1	Nylon	2.0	38.1	2.5	17.6	None	59	
C9	None	0.0	–	–	–	–		91
N2	Nylon	2.4	38.1	2.5	17.6	None		91
C10	None	0.0	–	–	–	–	51	154
N3†	Nylon	3.0	190	22	52.0	Yes	51	154

*Water : cement : sand ratio = 0.8 : 1.0 : 1.0.
†Fibres in beam longitudinal direction.

as the point where the instantaneous load/displacement ratio reduced to 95% of its original value. This method of finding the LOP point was adopted from an ASTM standard from the K_{Ic} test [24].

Typical load against load-line displacement curves are shown in Fig. 8 for CTS tests of different FRCs. The first curve for Mix K1 is plotted by starting at zero load and zero displacement. Displacements of successive mixes are plotted starting at increasing increments of 0.2 mm; this permits the drawing of multiple curves without excessive overlapping and/or enlargement.

The (apparent) critical stress intensity factor K_{Ic} for the CTS tests was also calculated from the specimen geometry and the LOP load, based on linear elastic fracture mechanics theory. As expected, the K_{Ic} value thus obtained was not valid as indicated by the stability of the fracture process during testing,

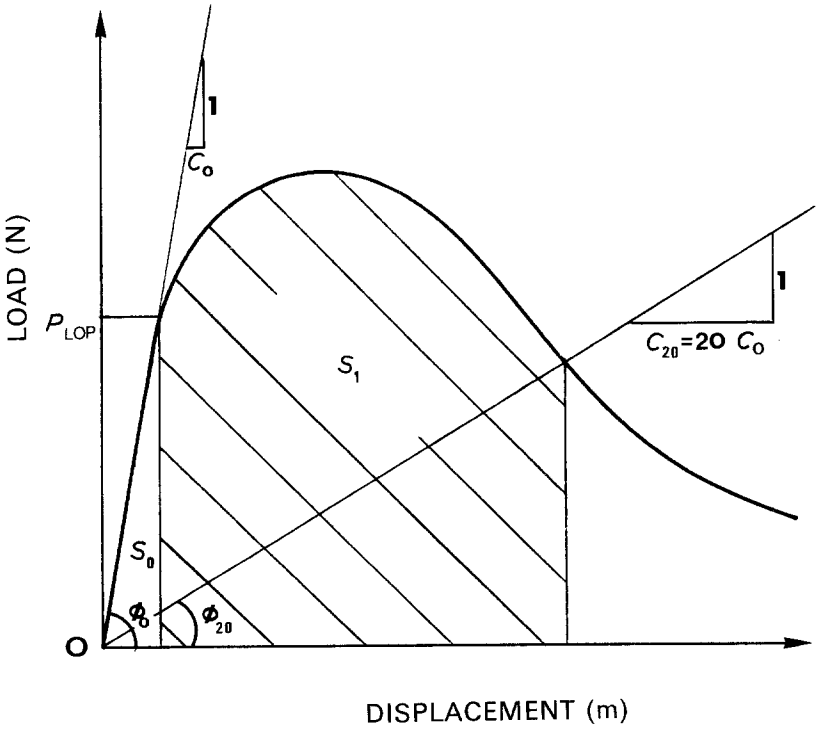

Figure 6 Definition of quantities for determination of T_0 and DTI_{20}.

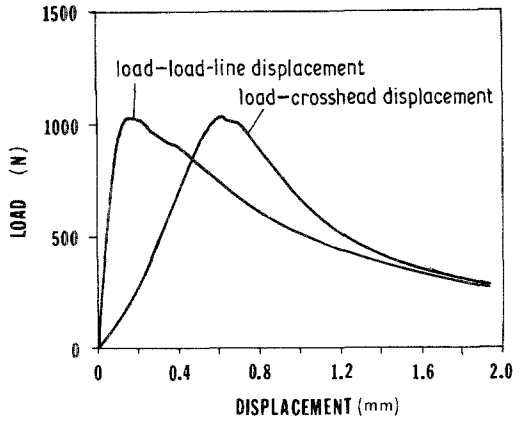

Figure 7 Test curves recorded for the same CTS specimen by two different means.

therefore it does not provide a meaningful measure of the toughness of FRC specimens. For these reasons, the calculated K_{Ic} is not included here. A procedure based on non-linear elastic fracture mechanics theory proposed by Li [25] and Li *et al.* [26] could be applied to deduce valid fracture toughness parameters for those FRC composites which exhibit a post-peak tension-softening behaviour. However, such a method requires measurements not included in this experimental programme.

In terms of the FRC toughness indicated by DTI_{20}, it is seen in Table IV that the aramid fibre reinforcement provides a very high toughness. The reason for this was that the aramid fibres were very strong and also formed a good bond with the matrix. Nylon FRC also showed greatly improved toughness properties, as seen from the DTI_{20} values. Because nylon formed a very weak bond with the matrix and the main reinforcing mechanism in nylon FRC was fibre pull-out, its toughness was mainly controlled by the fibre geometry and fibre distribution in the matrix.

The properties of FRC with acrylic fibres were quite different, because acrylic fibres were weak in strength but could form very strong bonds with the matrix. For FRC with long acrylic fibres the dominant reinforcing mechanism was fibre breakage. Note that for Mixes A6 and A7 shown in Table IV and Mix A6 in Fig. 8, the LOP toughness (T_0) and the first peak load was very high, but after the peak the load dropped rapidly so that the DTI_{20} was relatively low compared with other kinds of FRC. In another case when short-length fibres were used, such as for Mixes A4 and A5, both fibre breakage and fibre pull-out were important mechanisms after matrix cracking, and DTI_{20} for them was very high. The highest DTI_{20} was observed in Mix A3, for which great difficulties were encountered in the specimen fabrication process. This problem was not unexpected, since the fibre volume fraction for Mix A3 was 6.5%, much higher than for other FRC specimens. The matrix of Mix A3 appeared to have been weakened by excessive fibre inclusion and difficulties in filling the moulds, showing the lowest LOP toughness (T_0). This in turn tended to amplify the DTI_{20} which includes T_0 in its denominator.

It is noted in Table IV that the toughness of the specimens was improved even with reinforcement by fibres lying perpendicular to the loading direction (parallel to the loading holes) (Mix N3a), which was unexpected. Such an improvement actually reflects the effect of imperfect fibre alignment in the specimens. It is also interesting to note that the toughness of specimens with fibres lying in the loading direction (Mixes N3b and A8) was not higher than that for Mix N3a. This was because for most specimens in Mixes N3b and A8 the cracks turned and propagated along the fibre axial direction, often in the plane of a fibre layer.

As can be seen in Table IV, the toughness values T_0 and DTI_{20} show considerable variations. These variations were the direct reflection of the test records which in turn reflect the material property variations within a batch of specimens. Since the specimen size was of the same order of magnitude as the fibre lengths and the fibre distribution in the matrix was not directly controlled, these variations were not uncommon for the number of tests performed in this study.

4.3. Beam bending and splitting tensile tests

Four-point beam bending tests (Fig. 9) were carried out on a Model 1125 Instron machine at a crosshead speed of 0.25 mm min^{-1} (0.01 in min^{-1}). The mid-span deflection of the beam was measured by a clip gauge. A load–deflection curve was recorded by an X–Y plotter for each beam tested.

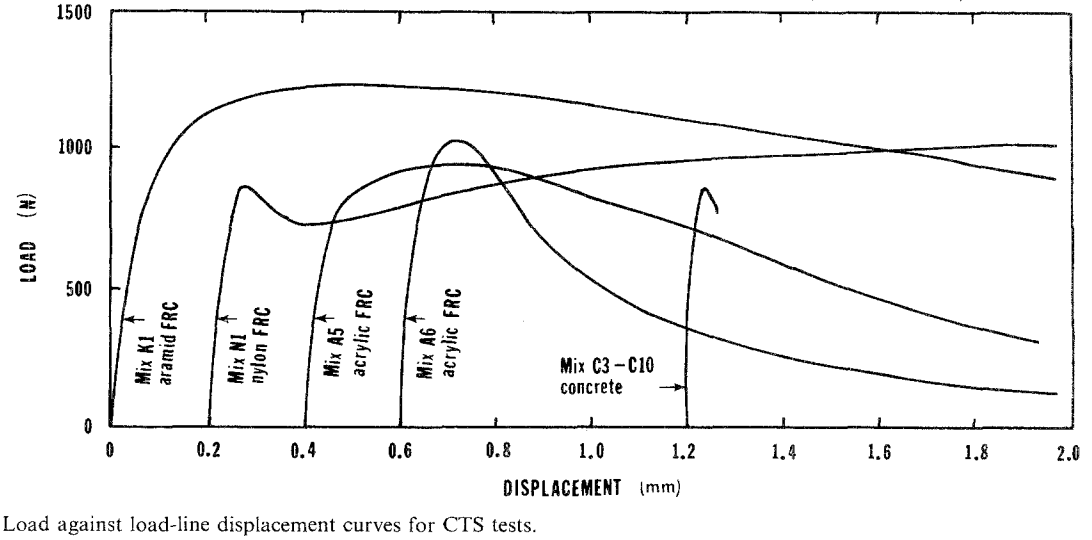

Figure 8 Load against load-line displacement curves for CTS tests.

TABLE IV CTS toughness

Mix No.	Fibre	V_f (%)	L_f (mm)	Number of tests	LOP Toughness		Toughness index	
					T_0 (N m m^{-2})	CV (%)	DTI_{20}	CV (%)
K1	Aramid	1.9	25.4	6	7.81	32.0	125.5	30.4
C3	–	0.0	–	5	5.53	38.8		
N1	Nylon	2.0	38.1	6	5.80	34.4	57.7	44.2
C8	–	0.0	–	6	5.43	16.8		
N3a	Nylon*	3.0	190	5	8.50	27.0	43.0	23.8
C10	–	0.0	–	6	5.78	17.4		
N3b	Nylon†	3.0	190	5	9.16	39.9	37.6	19.3
C10	–	0.0	–	6	5.78	17.4		
A4	Acrylic	2.0	6.4	5	4.80	18.3	79.1	30.0
C4	–	0.0	–	4	4.95	31.3		
A5	Acrylic	4.0	6.4	5	6.25	32.8	83.1	48.2
C4	–	0.0	–	4	4.95	31.3		
A3	Acrylic	6.5	6.4	6	3.99	52.0	181.3	27.1
A6	Acrylic	2.0	12.7	6	8.74	18.4	25.7	15.5
C5	–	0.0	–	6	5.34	16.3		
A7	Acrylic	2.0	19.1	6	11.11	18.2	32.4	14.1
C6	–	0.0	–	6	8.13	39.1		
A8	Acrylic†	4.5	Tow	5	7.87	30.7	19.0	46.0
C7	–	0.0	–	6	6.79	35.0		

*Fibres perpendicular to load direction, parallel to loading holes.
†Fibres parallel to load direction.

The nominal tensile stress in the beam bottom layer can be calculated from linear elastic beam theory as

$$\sigma = PL/BH^2$$

where P is the load (Fig. 9), L is the length of the beam (304.8 mm), B is the width of the beam (101.6 mm) and H is the height of the beam (101.6 mm).

Undamaged portions of beams which had been subjected to the bending tests were subsequently tested in a splitting mode using a Model 1125 Instron machine at a crosshead speed of 2.5 mm min^{-1} (0.1 in min^{-1}), as shown schematically in Fig. 10. Maximum loads were obtained from the load–time curves. The cracking splitting tensile stress is given by

$$\sigma = 2P/\pi BH$$

where P is the total maximum load (Fig. 10) and other quantities are the same as given for the flexural test.

The results of beam bending and splitting tensile tests are summarized in Table V and illustrated in Figs 11 and 12. Some flexural stress–strain (load–displacement) curves are shown in Fig. 13.

It was found that the LOP stress, the maximum stress, and the energy-absorbing abilities of concrete were improved by fibre reinforcement. By virtue of their high bond strength with cement matrix, acrylic fibres were more effective in improving the LOP stress of concrete in flexure than were nylon fibres, as indicated by Table V and Fig. 11. However, as can be seen from the test curves in Fig. 13, after the LOP point the load of the concrete reinforced with randomly distributed acrylic fibres (L_f = 19 mm) decreased rapidly, while the load of nylon FRC (L_f = 38 mm) could still increase and absorb more energy.

As seen in Fig. 13, the flexural behaviour of FRC beam specimens reinforced with continuous acrylic filaments lying in the beam longitudinal direction (Mix A8) was exceptional compared with other specimens. We have noted earlier in the case of Mixes A8 and N3b in CTS tests with fibres lying in the specimen loading direction that cracks developed parallel to the fibres and the resistance provided by the fibres was relatively small. In contrast, the structural constraints

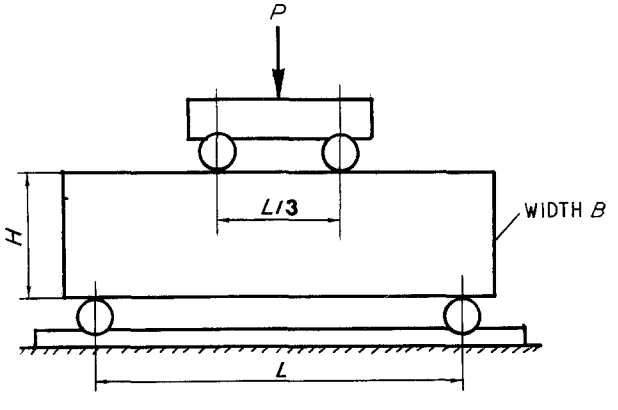

Figure 9 Schematic diagram for flexural tests.

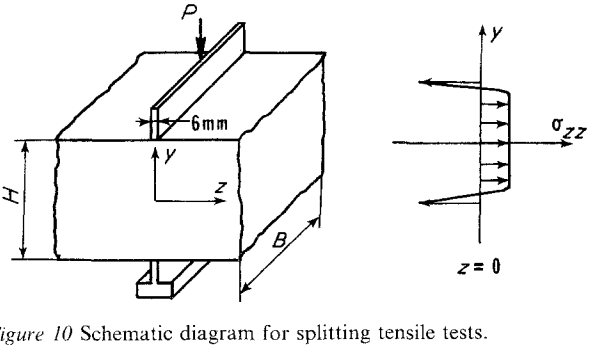

Figure 10 Schematic diagram for splitting tensile tests.

TABLE V Flexural and splitting tensile strengths

Mix No.	Fibre	V_f (%)	Flexural strength test					Splitting tensile test		
			LOP stress		Max. stress		No. of tests	Strength		No. of tests
			Average (MPa)	CV (%)	Average (MPa)	CV (%)		Average (MPa)	CV (%)	
C1	–	0.0	2.8	23.0	2.8	23.0	3	2.7	15.4	15
A1	Acrylic	2.4	4.6	4.4	4.6	4.4	4	3.3	5.8	23
C2	–	0.0	3.0	25.0	3.0	25.0	3	2.5	24.0	18
A2	Acrylic	2.4	5.8	8.7	5.8	8.7	5	3.3	9.7	23
C5	–	0.0	2.7	14.1	2.7	14.1	2	2.7	9.9	3
A6	Acrylic	2.0	4.8	11.2	4.8	11.2	4	2.8	8.8	8
C6	–	0.0	2.2	21.3	2.2	21.3	2	2.5	18.3	6
A7	Acrylic	2.0	4.2	5.4	4.5	6.2	4	2.5	7.0	9
C7	–	0.0	2.4	5.2	2.4	5.2	3			
A8*	Acrylic	4.5	6.3	13.9	14.7	10.3	3			
C9	–	0.0	2.7	18.5	2.7	18.5	3	2.7	20.8	7
N2	Nylon	2.4	3.9	18.5	6.6	15.6	5	2.2	12.9	8
C10	–	0.0	2.0	32.2	2.0	32.2	2			
N3*	Nylon	3.0	2.7	5.4	7.1	0.7	3			

*Continuous filaments in beam longitudinal direction.

of the flexural test prevented the failure mode of splitting between fibres; thus a very high post-elastic load was achieved, even at excessive beam deformations. Another factor which also contributed to this high load was that the fibre distribution in the aligned form permitted the inclusion of a relatively high fibre volume fraction (V_f = 4.5%).

In the splitting tensile test, the strength of FRC was found higher than that of plain concrete controls in some cases, but no significant difference in the strength between FRC and control specimens was observed in other cases. Even in the cases where the strength of FRC was found higher than that of concrete controls (Mixes C1 and A1, and Mixes C2 and A2), the increase in splitting tensile strength by fibre inclusion was only about one-third of the corresponding increase in the LOP stress observed in beam bending tests (Table V). It was also noted in these tests that all concrete control specimens failed suddenly with a loud cracking sound, but FRC specimens failed gradually and the matrix cracking sound was hardly recognizable. This observation confirms that even the inclusion of a small amount of fibres in concrete could significantly reduce the possibility of catastrophic failures, as indicated by the test curves beyond the LOP points.

5. Comments and conclusions

Small volume fractions of synthetic fibres (2 to 6.5%) mixed during preparation of a cement matrix have been shown to contribute significantly to specimen resistance to failure in a variety of standard mechanical tests. These include the compact tension test, the splitting tensile test, and the four-point beam bending test.

Four of the five synthetic organic fibres used in this experimental programme had initial moduli significantly below that of the concrete matrix. Further, the volume fractions V_f, of reinforcing fibres generally ranged from 2 to 4.5% with only one case of 6.5% V_f. Thus it was surprising to find significant increases for fibre-reinforced compared with non-reinforced concrete specimens in such measured properties as the LOP stress for the flexural test.

On the other hand, the positive influence of synthetic fibre reinforcement on maximum stress determinations or on designated failure energies (as in the case of the proposed DTI_{20} method) was not

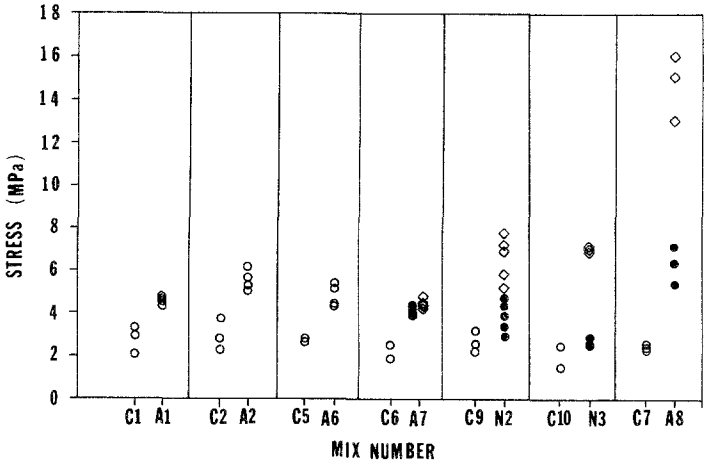

Figure 11 Results of the flexural tests. (○) LOP and maximum stresses, (●) LOP stress, (◇) maximum stress.

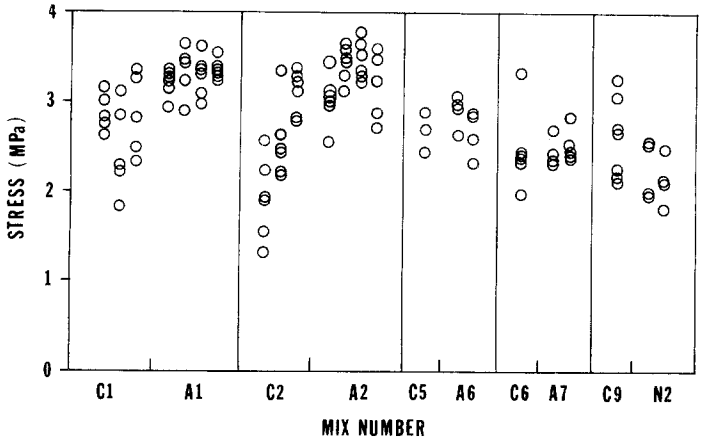

Figure 12 Results of the splitting tensile tests.

unexpected. Still, the magnitude of the reinforcing effect in certain tests was impressive. This was particularly noted in the CTS test, where the ratio of total energy to failure in reinforced compared with non-reinforced specimens was one to two orders of magnitude.

In contrast, while the maximum stresses calculated for the flexural test of the reinforced beam were always significantly higher than for the non-reinforced beam, they were not higher by an order of magnitude. Further, the maximum tensile stresses calculated for the splitting tensile test of the reinforced specimens on occasions manifested insignificant differences with reference to the control concrete specimens.

The questions raised by these experimental results provide a framework for further laboratory tests and theoretical studies. While the crack-bridging action of the synthetic fibres is manifested in the post-elastic region of the CTS tests, the contribution of the relatively low-modulus fibre in the elastic region is open to question, particularly as regards the approach to the limit of proportionality. The assumption of constant shear stress between fibre and cement matrix along the fibre length in the calculation of bond strength requires closer examination. Further, the distribution of fibres in the matrix warrants closer investigation, in that fibre clumping was often observed at the rupture surface. Also, more detailed scanning electron microscope examination of pulled-out fibre ends would be profitable for a better understanding of the pull-out mechanism which underwrites the remarkable increases in fracture energy of the FRC specimens. Likewise, a more detailed study of the effect of fibre length is desirable to define clearly the conversion from failure due to fibre pull-out to failure due to fibre rupture. The possibility of mixed fibre lengths should also be considered.

The fibres made available for this study were employed in the as-received state, with unknown surface finish. Considering the importance of the fibre–matrix interface in FRC mechanics, it follows that specification of the surface finish and even controlled modification on given fibre specimens will be an essential component of continuing laboratory studies. Likewise for other fibre parameters such as crimp and cross-sectional geometries, and for stress–strain behaviour as affected by draw ratio and heat relaxation.

Acknowledgements

The early part of this research programme has been supported by the E.I. du Pont de Nemours & Co. Inc., for which we express our appreciation. We acknowledge funding from the Shimizu Construction Co. Ltd,

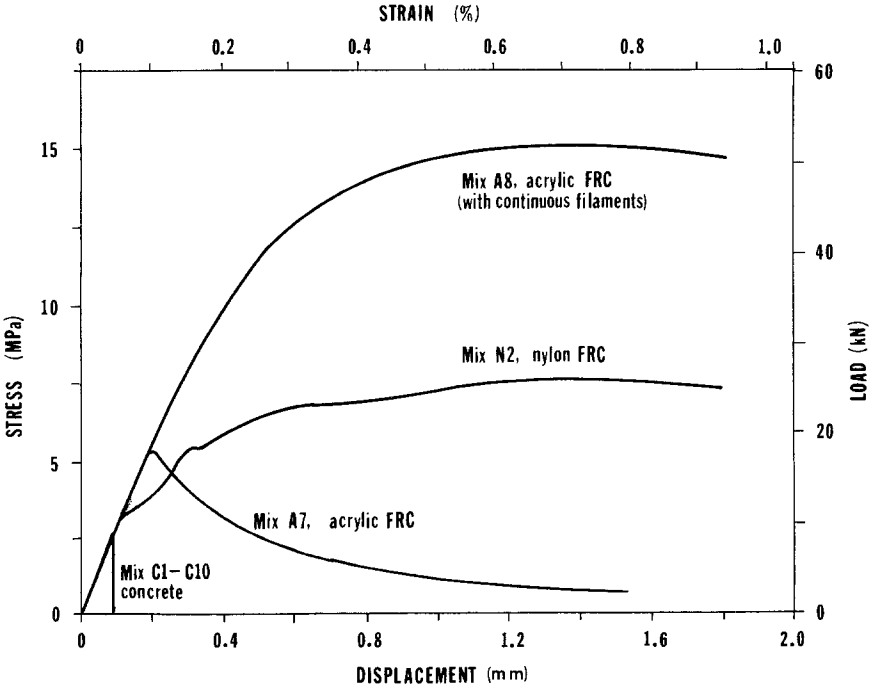

Figure 13 Typical flexural test curves.

Tokyo, and the National Science Foundation for the ongoing research programme.

References

1. J. B. SCALZI, paper presented at the Specialty Conference on Highway Infrastructures: Opportunities for Innovation, Leesburg, Virginia, July 1985.
2. C. E. STUBIG, "Highway Infrastructure: The Need to Balance Its Research Agenda", prepared as part of the 1985 Washington Internships for Students of Engineering (WISE) Program (1985).
3. H. G. KLOS, in "RILEM Symposium 1975: Fibre Reinforced Cement and Concrete" edited by A. Neville (Construction Press, Lancaster, 1975) p. 259.
4. ACI Committee 544, "State-of-the-Art Report on Fibre Reinforced Concrete", ACI 544.1R-82, ACI Manual of Concrete Practice, Part 5 (ACI, Detroit, 1986).
5. M. A. ALI, A. J. MAJUMDAR and D. L. RAYMENT, in "The Properties of Fibre Composites" Conference Proceedings, National Physical Laboratory (IPC Science and Technology Press, Guildford, Surrey, 1971) p. 27.
6. P. L. WALTON and A. J. MAJUMDAR, *J. Mater. Sci.* **13** (1978) 1075.
7. H. KRENCHEL and H. W. JENSEN, in "Fibrous Concrete" Symposium Proceedings, London, 1980 (The Construction Press, Lancaster, 1980) p. 87.
8. G. R. JAKEL, US Patent 3 899 344 (1975).
9. S. AKIHAMA, T. SUENAGA and T. BANNO, *Int. J. Cement Compos. Lightweight Concr.* **8** (8) (1986) 21.
10. ASTM Standard A 820: "Standard Specification for Steel Fibre Reinforced Concrete" (ASTM, Philadelphia, 1986).
11. ASTM Standard C 1018: "Test Method for Flexural Toughness of Fibre Reinforced Concrete (Using Beam with Third-Point Loading)" (ASTM, Philadelphia, 1986).
12. ACI Committee 544, "Guide for Specifying, Mixing, Placing, and Finishing Steel Fibre Reinforced Concrete", ACI 544.3R-84, ACI Manual of Concrete Practice, Part 5 (ACI, Detroit, 1986).
13. D. R. LANKARD, in "RILEM Symposium 1975: Fibre Reinforced Cement and Concrete" edited by A. Neville (Construction Press, Lancaster, 1975) p. 3.
14. J. F. RYDER, *ibid.* p. 23.
15. C. D. JOHNSTON, *Composites* **13** (1982) 113.
16. D. S. LYLE, in "Modern Textiles" (Wiley, New York, 1976) p. 44.
17. D. J. HANNANT, *Mag. Concr. Res.*, **35** (125) (1983) 197.
18. P. BARTOS, *Int. J. Cement Compos.* **3** (3) (1981) 159.
19. C. C. CHAMIS, "Mechanics of Load Transfer at the Fibre/Matrix Interface", NASA Technical Note: NASA TN D-6588 (NASA, Washington D.C., 1972).
20. S. MINDESS and J. F. YOUNG, "Concrete" (Prentice-Hall, Englewood Cliffs, N.J., 1981) p. 633.
21. ACI Committee 544, "Measurement of Properties of Fibre Reinforced Concrete", ACI 544.2R-78, ACI Manual of Concrete Practice, Part 5 (ACI, Detroit, 1986).
22. Y. WANG, SM thesis, Massachusetts Institute of Technology (1985).
23. Y. WANG and S. BACKER in preparation.
24. ASTM Standard E 399: "Test for Plane-Strain Fracture Toughness of Metallic Materials", (ASTM, Philadelphia, 1986).
25. V. C. LI, in "Application of Fracture Mechanics to Cementitious Composites", edited by S. P. Shah (Martinus Nijhoff, Dordrescht, 1985) p. 431.
26. V. C. LI, C. M. CHAN and C. LEUNG, *Cement Conc. Res.* **17** (1987) 441.

Received 18 November 1986
and accepted 27 April 1987